

Crawling, waving, inch worming, dilating, and pivoting mechanics of migrating cells: Lessons from Ken Jacobson

Alex Mogilner^{1,2,*} and Mariya Savinov¹

¹Courant Institute of Mathematical Sciences, New York University, New York, New York and ²Department of Biology, New York University, New York, New York

ABSTRACT Research on the locomotion of single cells on hard, flat surfaces brought insight into the mechanisms of leading-edge protrusion, spatially graded adhesion, front-rear coordination, and how intracellular and traction forces are harnessed to execute various maneuvers. Here, we highlight how, by studying a variety of cell types, shapes, and movements, Ken Jacobson and his collaborators made several discoveries that triggered the mechanistic understanding of cell motility. We then review the recent advancements and current perspectives in this field.

INTRODUCTION

Lamellipodial locomotion, in which a cell uses a wide, thin dynamic actomyosin network to crawl on flat surfaces, was the first mode of cell motility to be understood quantitatively (1–3). This understanding initiated, in no small part, due to several discoveries of Ken Jacobson and his collaborators. Ken was a leading cell biologist and biophysicist who pioneered novel (at the time) experimental techniques, such as fluorescence recovery after photobleaching (4) and chromophore-assisted laser inactivation (5). He was one of the earliest champions and adopters of computational modeling of cell dynamics (6) and was widely known for his studies of lipid and protein diffusion (7) and flow (8) in cell membranes.

Here, however, we focus on his insights into lamellipodial mechanics. Early observations (9) suggested that the cell propels itself by adhering the growing front of the lamellipodium firmly to the substrate and meanwhile using internal network contraction to retract the weakly adhesive lamellipodial rear. These observations raised a variety of mechanistic questions: how is the actin growth organized along the leading edge? How does the cell spatially grade its adhesion strength so that it is firm at the front and weak at the rear? How are the protruding front and retreating rear coordinated? Where and which forces does the cell apply to the substrate to move, and how can these forces control the di-

rection of motion? In the 1990s, Ken and his collaborators used fish keratocyte cells with rapid and steady lamellipodia to pave a way for answers to these questions. We discuss these relevant discoveries together with work of other researchers that, in sum, brought us to the current understanding of 2D motility. We then finish with a discussion of Jacobson's work relevant to 3D cell motility. Due to the brevity of this review, our focus is rather narrow, and we apologize for not mentioning many important studies.

Cell movements can be inferred from cell shape

A century ago, D'Arcy Thomson suggested that the diversity of biological forms can be explained by mechanics (10). On the cellular level, measuring forces and movements is much harder than observing shapes, so from the onset of cell motility research, the morphology of the cell shape, particularly of its leading edge, has been used to qualitatively describe a mechanical mode of cell migration (11). The first quantitative step in linking the leading-edge geometry of the migrating cell with the underlying cell mechanics was made by Lee et al. in 1993 (12). In that study, the authors posited the question: What are the protrusive movements behind the steadily advancing fan-like shape (Fig. 1 a) of the keratocyte leading edge?

The naive intuitive answer, based on the steady advancement of the leading edge, would be the *parallel extension model*: all regions along the cell margin advance with the same speed and direction. Lee et al., however, looked at

Submitted January 28, 2023, and accepted for publication March 15, 2023.

*Correspondence: mogilner@cims.nyu.edu

Editor: Meyer Jackson.

<https://doi.org/10.1016/j.bpj.2023.03.023>

© 2023 Biophysical Society.



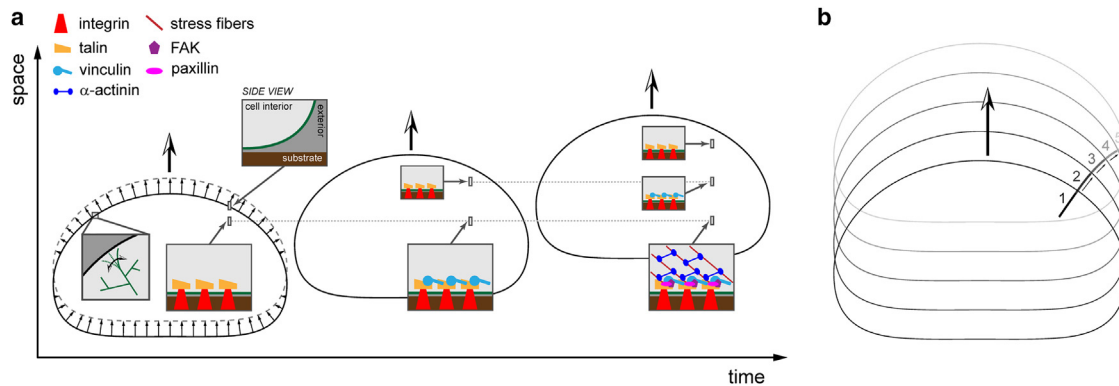


FIGURE 1 Mechanics, movements, and adhesions in cell migration. (a) Steady fan-like shape of a cell crawling with constant velocity evolving by graded radial extension: on the left, the solid contour outlines the lamellipodial boundary at an earlier point, while the dashed contour shows the boundary later. The arrows illustrate locally normal protrusions and retractions of the boundary, the rate of which decrease from the center to the sides of the cell edge. Left inset inside the leftmost cell illustrates why the protrusions are locally normal to the boundary: elastic actin filaments bend and tremble (*double arrow*) drumming on the leading-edge membrane, inflating it as if it was a rubber balloon. Three boundaries of the same motile cell are shown in the lab frame at three consecutive moments in time (left to right) as it moves through space (bottom to top). All remaining insets are side views of cell slices parallel to the direction of motion (see inset above leftmost cell, considering a slice at the leading edge), containing part of the bottom of the cell (*light gray*), the membrane (*green*), and the top layer of substrate (*brown*), illustrating the evolving chemical states of the adhesions at the actin-membrane-substrate interface. The simple nascent adhesion containing only integrin (*red*) and talin (*orange*) emerges early near the cell front (right inset inside leftmost cell). Individual adhesion complexes are stationary in the lab frame, so this same adhesion does not shift with time (*dashed lines*), as the cell front moves forward away from this adhesion and the rear gets closer to it. However, the chemical state of this adhesion evolves with time: after a while, vinculin (*light blue*) associates with the adhesion (larger inset of middle cell), and, finally, by the time the rear is close to the adhesion, paxillin (*pink*), FAK (*purple*), and α -actinin (*dark blue*) join, and stress fibers (*dark red*) form. This temporal evolution translates into the spatially graded adhesion (see the insets in the rightmost cell corresponding to the latest point in time), so that the chemically simplest adhesions are always near the leading edge, and the chemical complexity increases toward the cell rear. (b) Five consecutive contours of a steadily crawling (in the arrow direction) cell are shown together with the developing actin ridge. Nascent ridge 1 appears to the right from the center of the leading edge at the early stage. At stages 2–5, the ridge continues to grow in the locally normal directions to the corresponding current cell boundaries (numbers, small arrows, and lighter shading indicate consecutively grown segments of the ridge). According to the graded radial extension mechanism, the ridge bends to the right as it grows, as illustrated. To see this figure in color, go online.

lamellipodial “ridges” representing thickenings of the actin network within the lamellipodium (Fig. 1 b) and noticed that the closer these ridges were to the lamellipodial sides, the more they rotated outward (note that these ridges can be thought of as traces of the material points of the growing actin network). Individual ridges were also slightly curved, so that the ridge tip near the leading edge pointed outward in a perpendicular direction relative to the local outline of the edge, while the ridge end, deep within the lamellipodium and more proximal to the cell center, was more parallel to the direction of migration (Fig. 1 b). This finding is contrary to the parallel extension model but agrees with the *graded radial extension model*: the actin network protrudes in the locally normal direction relative to the leading edge (Fig. 1 a). But then, simple trigonometry necessitates that the local protrusion rate is not constant, as in the parallel extension model, but is spatially graded: the more the leading edge curves backward as one goes from the front to the side, the slower the protrusion rate (Fig. 1, a and b). Lee et al. then turned this result around and proposed that it is not the shape that determines the protrusion rate, but rather the grading of the protrusion rate determines the shape.

The next logical questions are: Why are the local protrusions pushing perpendicular to the cell boundary, and what regulates the protrusion rate grading in space? The answer to the first question is given by the polymerization ratchet

models of protrusion (13): thermally “trembling” actin filaments at the edge of the growing lamellipodial network “drum” on the plasma membrane from the inside, much like air molecules drum on the inside surface of a rubber balloon, effectively creating a pressure that stretches the membrane locally normal to the edge (Fig. 1 a). Grimm and co-workers (14,15) suggested the answer to the second question: the cell concentrates more actin at the center of the front and the network density decreases toward the sides, so the effective pressure becomes gradually weaker away from the center and thus the membrane is pushed slower there.

The study of Lee et al. (12) eventually inspired examinations of how the whole cell shape, not just of the leading edge, is regulated by the growth and deformation of the lamellipodial actin network. Several models demonstrated that varying simple phenomenological rules of switching between protrusion and retraction along the whole cell edge can reproduce most of the observed shapes and movements of many types of cells (16,17).

A mechanistic explanation of the whole lamellipodial shape emerged from (18): in the moving cell, myosin in the lamellipodium is swept to the rear, where it generates contraction. The geometric sum of the spatially graded actin growth (faster at the front, slow at the sides) and actomyosin contraction (faster at the rear, slow at the sides) then also reproduces the moving lamellipodial shapes. Not only

lamellipodial shapes can be explained mechanistically: many slowly migrating cells, like fibroblasts, exhibit long parts of their perimeter arching inward. Normally, there are tensed stress fibers running along these perimeter parts. The cell edge curvature can then be explained by the Laplace law: membrane tension pulling the boundary inward is balanced from the inside by the stress fiber tension, which is generated by myosin contraction and elastic deformations (19).

Overall, quantitative links between cell shape and movements were proven to be universal, not only limited to keratocytes and fibroblasts. The increase in cell speed and persistence was shown to coincide with a transition between cell shapes and migration modes across many cell types (20). For example, higher speeds generally correlate with broader cells (21). While cell shape informs about the mechanics of motility, it also informs about guided migration in response to directional cues: chemotactic *Dictyostelium discoideum* cells are rounder and have numerous split protrusions in shallow chemical gradients, while more polarized “wedge” shapes emerge in steep chemical gradients (22). Modeling suggests that the rounder multiprotrusion shape allows the cell to sense weak noisy chemotactic signals better, while the polarized uniprotrusion shape accounts for more effective migration when the migration direction is unambiguous (22).

Adhesion turnover translates into spatially graded adhesion for rapid cells

Adhesion is as important as protrusion and retraction for effective cell motility: without mechanical coupling to the substrate, protrusion and retraction would just cause a treadmill of the lamellipodial network with no net displacement. Intuitively, adhesion must be mechanically firm at the front to prevent the growing network pushing against the leading-edge membrane from sliding backward, and weak at the back to not hold up the retracting cell rear. Indeed, such graded adhesion has been observed (23–25) and theoretically predicted (26) in early studies. So, how can adhesion be graded in this fashion?

Microscopy of the molecular adhesion complexes revealed consecutive spatial layers of different proteins (27), suggesting sequential assembly of the adhesions in precise molecular order. Research on individual adhesion dynamics (reviewed in (3)) confirmed that this is the case. First, integrins spanning the membrane and connecting the actin network to the outside environment make small aggregates. Almost immediately, talins (links between actin and integrins) appear. Then, vinculins (important mechanosensors) get added, followed by cross-linkers, signaling molecules, and other adaptors (3). These molecular events are synchronized with changes of shape of the adhesion complexes, and, more importantly, of the adhesive mechanical properties. Some adhesions turn over rapidly, while others stabilize

and mature but eventually age and fall apart as well. The attractive hypothesis is that the mechanical strength of the adhesions is a function of molecular complexity, so how firm an adhesion complex is, depends on the stage of its molecular turnover cycle. In slowly moving cells, these adhesion turnover cycles are faster than the characteristic migration timescale, and the relation between these cycles and the grading of the adhesion strength on the scale of the whole cell is not apparent.

On the other hand, rapid keratocytes offer a very interesting way to connect the temporal adhesion turnover cycle to the spatially graded adhesion cycle (Fig. 1 a). Jacobson’s group observed that, in these cells, integrin and talin molecules were localized within a narrow rim of nascent adhesions along the leading edge (Fig. 1 a, left). These molecules were joined by vinculin in adhesions distributed evenly throughout the lamellipodium (Fig. 1 a, middle). Also, α -actinin, an important cross-linker, was found in adhesions at the rear (28) (Fig. 1 a, right). The authors concluded then that rapid locomotion converted the temporal adhesion evolution cycle into a spatial one, providing the adhesion complexes do not shift on the substrate (which was also observed). First, the “youngest,” molecularly simple adhesions emerge under the nascent, most recently, grown actin network at the front. Then by the time vinculin joins, the leading edge has moved past the “older” adhesions, and finally by the time the next molecules associate with the adhesion complexes, the “aged” adhesions approach the retreating rear edge of the cell (Fig. 1 a).

This pioneering paper set the stage for more precise characterization of the temporal-spatial coupling of the adhesion cycles (29). It is tempting to hypothesize that the young nascent adhesions at the front are firmer than the mature adhesions at the rear, setting the optimal conditions for the mesenchymal migration, but so far there is no direct evidence of this. One of the best supports for this hypothesis is a recent elegant study (30). Its authors demonstrated that cells apply forces to the substrate, which gradually rupture local ligands, creating a gradient of ligand surface density underneath the cell: more ligands under the leading edge and fewer under the rear. By the time the rear approaches a local adhesion, the local ligands are ruptured within the time needed to advance the cell body. The authors of (30) demonstrated that this ligand gradient in turn drives and guides the cell migration. Note that the graded adhesion mechanism proposed in (30) relies not on adhesion molecular complexity, as in (28), but on the abundance of ligand molecules on the surface to which integrins bind.

Many mechanisms for weakening and/or releasing adhesions at the rear, other than the hypothesized aging-weakening coupling mentioned, were discovered to work in both rapidly and slowly migrating cells. First, in polarized migrating cells, different chemical or structural conditions at the front and rear can be harnessed to release adhesions at the rear. For example, a polarized phosphoinositide

pattern upregulates endocytosis of adhesion molecules in a moving cell's rear (31). Another possibility is that frequent contacts with dynamic microtubules weaken the adhesions, as mature adhesions at the back of migrating cells were observed to be targeted by a dense microtubule array (32). Second, since adhesion properties are force sensitive (33) and the contractile forces applied to the adhesions are often stronger at the rear of the crawling cell (34), cells can in principle spatially regulate the adhesions. However, there is a poorly understood tension-dependent *molecular switch* from adhesion assembly to maturation and disassembly (35), which likely relies on several respective mechanisms, for example, on upregulation of the recruitment of calpain by the myosin-generated contractility (36), which mediates proteolysis of a few types of adhesion molecules (37). There is also indirect evidence that higher myosin contraction induces a *mechanical switch* from firm “sticking” to weak “slipping” adhesions (38).

In fact, Jacobson's group discovered a complex and elegant force-dependent mechanism of releasing adhesions at the back of migrating cells by observing inch worming motility (39) of normally steadily crawling keratocytes. Occasionally, the observed rapid fan-shaped cells had a large unreleased adhesion at the rear, and this rear point became stuck, so a long narrow tail developed behind slowing wide front, resulting in a characteristic fibroblast-like shape. This stuck state, however, was transient—after a while, the tail snapped, and the rear caught up with the accelerating front. Lee et al. (39) found that, as the cell elongated, tension increased across the cell. When the tension exceeded a critical threshold, stretch-activated calcium channels in the membrane were activated, triggering an influx of extracellular calcium and a subsequent release of calcium from intracellular stores. The calcium increase, through a variety of mechanochemical pathways, then activated various local adhesion detachment mechanisms (40). Upon the release of the rear adhesion, the tension decreased after retraction, restoring the cell propulsion and shape.

Distribution of propulsive, pinching, and frictional traction forces is a signature of motility mode

Myosin-generated active contractile forces inside migrating cells, partially dampened by passive viscoelastic deformations of cytoskeleton, are applied to the substrate, enabling the cell to move. Measuring the cytoskeletal active and passive forces is extremely difficult (41), but traction force microscopy allows one to measure the forces the cell applies to the substrate by inferring the elastic stresses in flexible substrates from measurements of substrate deformations underneath and at the sides of the motile cell. This then allows us a glimpse at the distribution of forces inside the cell and at the design of the motile machinery. Jacobson and collaborators used one of the earliest applications of traction force mi-

croscopy to understand the cell crawling mechanics (42). These mechanics are based on the balance of propulsive and frictional forces: the cell can adhere to the substrate firmly at the leading edge and pull inward, thus applying a rearward force to the substrate. By the third Newton's law, the substrate in turn applies a forward (propulsive) force to the cell. This propulsive action drags the cell body forward, so there is also a frictional force between the substrate and the cell body. In this example, the propulsive/frictional pair of forces behave as a so-called force dipole with propulsion at the front and friction in the middle to rear of the body. Note that the geometric sum of all force vectors applied to the substrate has to be equal to zero, because the opposing traction forces result from balanced (again, by the third Newton's law) forces inside the cell. Alternatively, the force dipole can be with propulsion at the rear, if, instead of pulling at the leading edge, the cell pushes the substrate backward with its rear. These examples illustrate how knowing where the forces are applied to the substrate can inherently reveal the mechanical design of the crawling cell.

However, Oliver et al. measured the traction forces under the steadily crawling keratocytes (42) and did not find any obvious propulsion or frictional forces (Fig. 2 a). Instead, they observed strong “pinching” forces at the distant sides of the cell directed inward perpendicularly to the front-rear axis (Fig. 2 a, *second cell from top*). (Note, that in the figure we show the forces applied by the substrate to the cell, which are opposite to the traction forces described here.) It is intuitive that a crawling action cannot result from the pinching, so where were the propulsion and friction? The crucial hint came from the cells with transiently stuck tails, as in (39). In such cells, instead of the pinching force dipole at the sides, a more complex force triplet emerged at the tail and at the sides of the leading edge (Fig. 2 a, *bottom*). The forces applied by the cell to the substrate at the tail were directed forward (as such, frictional). At the frontal sides, instead of being directed perpendicular to the direction of motion as in pinching, the forces were directed at an angle both to the frontal center and backward, thus combining pinching and propulsive forces (Fig. 2 a, *second cell from bottom*). The authors then suggested the solution to the puzzle: normally, in steadily crawling keratocytes, the propulsion and frictional forces are applied throughout the lamellipodium, so they locally almost cancel each other and are thus hard to detect (Fig. 2 a, *top*) (“almost” is crucial; complete cancellation would make crawling impossible). But when the rear gets stuck, the propulsion and friction segregate transiently.

The explanation for why the pinching forces are so strong in keratocytes is elucidated through modeling of the internal forces (18). Myosin contraction in the rear half of the lamellipodium is muscle-like: the longer the chains of the myosin contractile units are, the faster the muscle-like contraction is at the ends, and then the stronger the inward pulling is at the

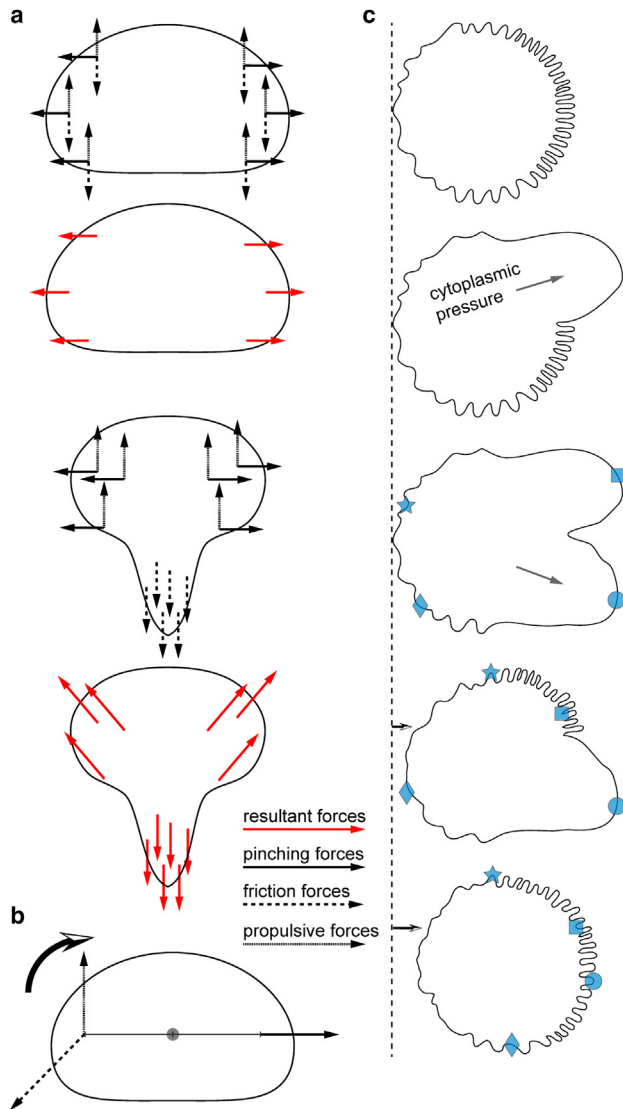


FIGURE 2 Forces and movements in migrating cells. (a) Forces exerted on the cell by the substrate (equal and opposite to traction forces exerted on the substrate by the cell) are shown with arrows. Top two cells: pinching forces (*solid*) pull the cell sides apart. The propulsive forces (*dotted*) pull the cell forward and are resisted by equal and opposite friction forces (*dashed*). Because the propulsive and friction forces are applied in roughly similar locations in the steadily moving cell, the resulting forces (*red*) detected in experiments are pinching forces only. Bottom two cells: when the cell rear gets transiently stuck, propulsive and friction forces are segregated to the front and rear, respectively, resulting in experimentally detected forces (*red*) that exhibit propulsive and friction elements in addition to pinching. (b) In the cell turning clockwise (*arrow*), the left-right force symmetry is broken: most of the pinching force is concentrated at the slow (*right*) side of the cell, while most of the propulsion and frictional forces are concentrated at the fast (*left*) side. Note that the pinching force does not exert a torque on the cell relative to the cell center (*dark spot*), while the propulsive force generates the clockwise active torque, balanced by the counterclockwise passive torque from the friction force. Note also that the total vector sum of all forces here and in the steady case (a) are equal to zero. (c) Consecutive cell contours from top to bottom show one cycle of the dilation-compression motility mechanism. Initially (*top*), the myosin action has already compressed and folded the membrane and cortex of the future cell front. Then, the cytoplasmic pressure dilates and unfolds

ends. Crawling keratocytes are very long from side to side, with long myosin chains, hence the great pinching forces. Indeed, the proportionality of the net traction force magnitude to the length (43) and area (44) of cells other than keratocytes was experimentally demonstrated, although the mechanisms consist of not just physical scaling but also complex mechanochemical feedbacks involving adhesion dynamics. An interesting question is: what is the physiological role for the strong pinching forces? Oliver et al. proposed that such forces could peel away rear adhesions like an adhesive tape pulled from the edge (42). Another interesting idea in (42) is that large traction forces are not necessary for locomotion and that strong pinching forces are developed instead for remodeling extracellular matrix and organizing the epithelial layer. Indeed, cells without specific molecular adhesions to the substrate (but still interacting with it through physical forces) can migrate rapidly while developing traction forces several orders of magnitude lower than during the adhesion-based motility (45). Curiously, these cells also developed the inverted force dipole: the propulsion forces were found in the rear, while the frictional forces were in the middle and front.

The study of Oliver et al. (42) triggered investigations of the traction forces in other cell types. In fibroblasts, the traction forces were discovered to be applied to discrete focal adhesions at the ends of stress fibers at the periphery (46), while forces applied to the cell body at the opposite ends of the stress fibers moved the cell body (47). In contrast, in keratocytes, the cell body appears to simply ride on top of the lamellipodium. One of the greatest insights came from measurements of the traction forces and flow rates of the actin network simultaneously (38,48–50). These simultaneous measurements are the only way to estimate the mechanical properties of adhesions because the local ratio between the traction force and actin speed can be interpreted as the effective adhesive drag. These estimates revealed the widely common property of a stick-slip adhesion transition, mentioned above.

Measurements of traction forces were followed by efforts to measure intracellular forces. Broadly speaking, two types of approaches to intracellular mechanics emerged. One is based on inferring the forces inside the cell from spatial-temporal fluctuations in cytoskeletal networks (41) or the

the cortex-membrane, creating one protrusion, and then another. At this stage (*middle*), we mark four material points on the cell boundary by square and circle on the front, and diamond and star on the rear. Next, one of the sides of the cell front compresses and folds, which leads to slight retraction of that front portion (*square*) but significant advancement of the adjacent rear (*star*). Finally, the remaining part of the cell front compresses and folds, which leads to slight retraction of the protrusive part (*circle*) and significant advancement of the adjacent rear (*diamond*). During each such motility cycle, the dilation-compression wave spans the leading edge back-and-forth once, and the cell advances (arrows near the dashed line delineating the distance from initial rear position). To see this figure in color, go online.

cytoplasm (51). Another method is based on engineering proteins with fluorophore pairs, so that force-induced deformations in the protein impact the separation distance between fluorophores, causing the FRET fluorescent signal to vary as a function of force. Such force probes have been developed to sense the tension in, for example, vinculin (52) and α -actinin (53), and, when expressed in living cells, to provide measurements of the intracellular forces. So far, the results from both approaches reveal intracellular forces to be rapidly fluctuating both in time and in space (41) and not being correlated in a simple way with cells' shapes and movements (53).

Mechanical and biochemical asymmetries allow cells to turn

In several experiments measuring keratocyte traction forces, Oliver et al. observed keratocytes executing a sharp turn (42). For such cells, there was a stronger pinching force at the slow side (Fig. 2 b), but the sidewise pinching force is unlikely to contribute to the cell change of direction. More importantly, there was a stronger propulsion in the faster, pivoting side (Fig. 2 b). This makes sense mechanically—stronger and more frequent pulls on the left side of the cell front will result in the cell turning right. Note that the authors of (42) discussed the cell mechanics as if the cell can be considered a rigid (or elastic) body. The *total torque* on the rigid cell body then must be equal to zero (because the inertial and fluid viscous torques are negligibly small), so the active part of the torque, generated by the propulsion, is exactly balanced by the passive part of the torque caused by friction (Fig. 2 b); the direction of turning is then defined by the active, propulsive part of the torque.

Recently, Allen et al. reexamined turning keratocytes by measuring, in addition to the traction forces, the flow of the lamellipodial actin network relative to the substrate and cytoskeletal asymmetries in the pivoting lamellipodium (54). The most significant revision of the scenario proposed in (42) is that, on the relevant timescale of minutes, the lamellipodium is more adequately represented by a highly viscous fluid body with free boundaries (where the physical boundary of the actin network grows at the front and shrinks at the rear). The turning then relies on the following positive feedback: in the framework of the pivoting cell, myosin is left behind and slightly biased to the fast side. This leads the rear of the fast side to retract quicker, effectively pivoting the rear long axis of the cell, so the kinematic act of turning and asymmetric myosin contraction reinforce each other, locking the cell in the turning state. Curiously, the leading-edge orientation and direction follows the rear axis of the cell, so the cell effectively turns from the rear.

In addition to mechanics of the turning mechanism described in (54), one can expect that additional biochemical regulatory pathways govern cell turning. Jacobson's group illustrated the design of one such mechanism in a

tour-de-force experiment (55) that preceded current powerful optogenetics approaches (56). Roy et al. locally uncaged protein thymosin β 4 in one of the sides of a rapidly, directly, and steadily crawling symmetric cell (55). The photoreleased thymosin β 4 then rapidly sequestered actin monomers in the cytoplasm at the cell side. This resulted in an immediate dramatic cell turn toward the direction of photoactivation; the cell effectively pivoted around the irradiated region. Both protrusion and contraction were inhibited at one of the cell wings, and the irradiated wing became a pinned down anchor, around which the opposite unaffected wing pivoted, held on a circle by the cell membrane connecting the effective anchor and the active wing. Thus, asymmetric (between left and right relative to the direction of migration) distribution of regulatory molecules is another mechanism of turning, likely complementing the mechanical pivoting. Another hint at the biochemical turning regulation is the observation of left-right asymmetry in the frequency of calcium sparks between the two halves of the lamellipodium of turning keratocytes, which pivot about the side with the greater number of sparks (57).

So far, we have discussed smooth pivoting of a single lamellipodium. This turning mechanism is likely limited to simple-shaped rapidly moving cells. Slow, irregularly shaped, cells change direction by either laying down focal adhesions (58) and/or F-actin bundles (59) at the side of the prospective turn, and then developing a protrusion using these adhesions and actin bundles as rails. Internally, the direction of the turn is controlled by spatially regulated Rho GTPase activation (58,60). Directional changes induced by environmental cues, in many cases, are executed as a result of competition between multiple protrusions-pseudopods extending not only from the front but also from the cell sides (and in some cases, the protrusions branch out from each other) (60–62). Governed by intracellular signaling networks interpreting extracellular cues, protrusions in a new direction grow and “win,” while protrusions on the former front and other sides wither.

Looking forward: From 2D to 3D

Thus far we have focused on mesenchymal cell motility characteristic of cells moving on stiff 2D surfaces. In the last decade, much research has reoriented to start investigating motility in 3D environments, for example, cells migrating through the extracellular matrix (63). Lamellipodial protrusions are observed in 3D environments too (64–66), but often ameboid motility emerges (67) in which actomyosin cortex contraction, stronger in the cell rear than at the front, does two things. The first is increasing hydrostatic pressure in the cell that causes the breakage of cortex-membrane links at the front and inflating a membrane “bubble,” the so-called bleb (64). The bleb pushes the cell front forward, followed by reassembly of the actomyosin cortex at the leading-edge membrane. Secondly, the asymmetric

cortex contraction is pulling most of the actomyosin cortex to the rear, so that the rearward flow of the cortex generates effective friction against the cell's surroundings, which then propels the cell forward (68).

Jacobson's group discovered another cell protrusion mechanism in 3D—dilation/compression (69) (Fig. 2 c). What they observed was, on the first glance, very similar to a bleb. However, in a bleb the plasma membrane extends outward from the cell margin first, and only later the actomyosin density at the new cell boundary increases to a baseline. Kapustina et al. noticed that, on the contrary, the plasma membrane extended outward in synchrony with the actomyosin density, so the thin cortex and the underlying plasma membrane protrude together (69). The cortex normally is either quiescent or contractile, so it is hard to understand how it can expand; similarly, the lipid membrane is inextensible. The essence of the novel protrusion became clear from high-resolution microscopy: the membrane of the cell surface is not pulled taut but folded, with microscopic folds effectively “stapled” together by the actomyosin cortex. The dilation (protrusion) happens when the cytoplasmic pressure stretches the membrane enough to overcome the folding action of the cortex (Fig. 2 c, *second from the top*). When the pressure is not enough (or actomyosin contraction is weak), the contraction of the cortex and cross-linking leads to the membrane folding, which reduces the volume of the cytoplasm covered by the folded part of the membrane and local retraction of the cell boundary (Fig. 2 c, *bottom*). This study demonstrates that multiple and redundant, physically diverse mechanisms can be responsible for the “bleb-like protrusion” in 3D.

Cellular turning mechanisms are probably also more diverse in 3D than 2D. Recently, it was observed that cells in complex environments alternate persistent, relatively straight, run phases with tumble phases that result in cell re-orientation (64), much like in flagella-driven bacterial swimming motility. Runs are characterized by the formation of directed actin-rich protrusions and tumbles by enhanced blebbing.

Many concepts and lessons learned from the 2D motility are applicable in 3D, even in collective cell migration. Simply observing the shape of pseudopods informs us about the motility mechanisms. For example, blunt cylindrical lobopodia point to pressure-driven protrusions versus flat and thin lamellipodia, which indicate actin-based pushing at the leading edge (63). Shapes of cells in groups also allow us to reverse-engineer intercellular forces (70). Measuring where traction forces are applied, similarly to 2D, allows us to infer how intracellular forces propel the cells in 3D and collective groups (71). For example, recent measurements of the traction forces in zebrafish tissues led to the realization that the rear of the collectively migrating primordium cell group exerts higher contractile stresses than the front, suggesting that this tissue pushes itself forward with its back (72). Simply measuring the magnitude of the trac-

tion forces turned out to be very useful, but the results point again to extreme diversity in migration mechanisms in 3D. For example, the measured traction forces are often great in 3D cancer invasion (73), suggesting strong contraction and adhesion. On the other hand, instead of large focal adhesions, diffuse adhesion proteins and very rapidly turning over small adhesions were observed in 3D (74), suggesting that the role of specific molecular adhesions is lesser. In the extreme case, cells can even self-propel in 3D with the complete absence of adhesion, just by harnessing viscous forces generated by rearward membrane flow, tangential to the cell-liquid interface when immersed in fluid (75). Much effort will be needed to reach a truly quantitative understanding of the 3D motility, because 3D imaging so far is very inferior to the great microscopy and micromanipulation tools in 2D that allowed Ken Jacobson and other leaders of the cell motility community to elucidate the migration mechanisms.

AUTHOR CONTRIBUTIONS

A.M. and M.S. conceived and wrote the manuscript.

ACKNOWLEDGMENTS

We thank A.F. Horwitz for useful discussions. We were supported by NSF grants DMS 2052515 and DMS 1953430.

DECLARATION OF INTERESTS

The authors declare no competing interests.

REFERENCES

1. Svitkina, T. M., A. B. Verkhovsky, ..., G. G. Borisy. 1997. Analysis of the actin-myosin II system in fish epidermal keratocytes: mechanism of cell body translocation. *J. Cell Biol.* 139:397–415. <https://doi.org/10.1083/jcb.139.2.397>.
2. Pollard, T. D., and G. G. Borisy. 2003. Cellular motility driven by assembly and disassembly of actin filaments. *Cell.* 112:453–465. [https://doi.org/10.1016/S0092-8674\(03\)00120-X](https://doi.org/10.1016/S0092-8674(03)00120-X).
3. Gardel, M. L., I. C. Schneider, ..., C. M. Waterman. 2010. Mechanical integration of actin and adhesion dynamics in cell migration. *Annu. Rev. Cell Dev. Biol.* 26:315–333. <https://doi.org/10.1146/annurev.cell-bio.011209.122036>.
4. Jacobson, K., Z. Derzko, ..., G. Poste. 1976. Measurement of the lateral mobility of cell surface components in single living cells by fluorescence recovery after photobleaching. *J. Supramol. Struct.* 5:565(417)–576(428). <https://doi.org/10.1002/jss.400050411>.
5. Jacobson, K., Z. Rajfur, ..., K. Hahn. 2008. Chromophore-assisted laser inactivation in cell biology. *Trends Cell Biol.* 18:443–450. <https://doi.org/10.1016/j.tcb.2008.07.001>.
6. Weinreb, G. E., T. C. Elston, and K. Jacobson. 2006. Causal mapping as a tool to mechanistically interpret phenomena in cell motility: application to cortical oscillations in spreading cells. *Cell Motil Cytoskeleton.* 63:523–532. <https://doi.org/10.1002/cm.20143>.
7. Jacobson, K., P. Liu, and B. C. Lagerholm. 2019. The lateral organization and mobility of plasma membrane components. *Cell.* 177:806–819. <https://doi.org/10.1016/j.cell.2019.04.018>.

8. Lee, J., M. Gustafsson, ..., K. Jacobson. 1990. The direction of membrane lipid flow in locomoting polymorphonuclear leukocytes. *Science*. 247:1229–1233. <https://doi.org/10.1126/science.2315695>.
9. Abercrombie, M., J. E. Heaysman, and S. M. Pegrum. 1970. The locomotion of fibroblasts in culture I. Movements of the leading edge. *Exp. Cell Res.* 59:393–398.
10. Thompson, D. A. W. 1942. *On Growth and Form*, 2nd edition. Cambridge University Press.
11. Trinkaus, J. P. 1973. Surface activity and locomotion of *Fundulus* deep cells during blastula and gastrula stages. *Dev. Biol.* 30:69–103.
12. Lee, J., A. Ishihara, ..., K. Jacobson. 1993. Principles of locomotion for simple-shaped cells. *Nature*. 362:167–171. <https://doi.org/10.1038/362167a0>.
13. Mogilner, A., and G. Oster. 1996. The physics of lamellipodial protrusion. *Eur. Biophys. J.* 25:47–53. <https://doi.org/10.1007/s002490050016>.
14. Grimm, H. P., A. B. Verkhovskiy, ..., J.-J. Meister. 2003. Analysis of actin dynamics at the leading edge of crawling cells: implications for the shape of keratocyte lamellipodia. *Eur. Biophys. J.* 32:563–577. <https://doi.org/10.1007/s00249-003-0300-4>.
15. Keren, K., Z. Pincus, ..., J. A. Theriot. 2008. Mechanism of shape determination in motile cells. *Nature*. 453:475–480. <https://doi.org/10.1038/nature06952>.
16. Satulovsky, J., R. Lui, and Y. I. Wang. 2008. Exploring the control circuit of cell migration by mathematical modeling. *Biophys. J.* 94:3671–3683. <https://doi.org/10.1529/biophysj.107.117002>.
17. Raynaud, F., M. E. Ambühl, ..., A. B. Verkhovskiy. 2016. Minimal model for spontaneous cell polarization and edge activity in oscillating, rotating and migrating cells. *Nat. Phys.* 12:367–373. <https://doi.org/10.1038/nphys3615>.
18. Barnhart, E. L., K.-C. Lee, ..., J. A. Theriot. 2011. An adhesion-dependent switch between mechanisms that determine motile cell shape. *PLoS Biol.* 9:e1001059. <https://doi.org/10.1371/journal.pbio.1001059>.
19. Labouesse, C., A. B. Verkhovskiy, ..., B. Vianay. 2015. Cell shape dynamics reveal balance of elasticity and contractility in peripheral arcs. *Biophys. J.* 108:2437–2447. <https://doi.org/10.1016/j.bpj.2015.04.005>.
20. Maiuri, P., J.-F. Rupprecht, ..., R. Voituriez. 2015. Actin flows mediate a universal coupling between cell speed and cell persistence. *Cell*. 161:374–386. <https://doi.org/10.1016/j.cell.2015.01.056>.
21. Wortel, I. M. N., I. Niculescu, ..., J. Textor. 2021. Local actin dynamics couple speed and persistence in a cellular Potts model of cell migration. *Biophys. J.* 120:2609–2622. <https://doi.org/10.1016/j.bpj.2021.04.036>.
22. Tweedy, L., B. Meier, ..., R. G. Endres. 2013. Distinct cell shapes determine accurate chemotaxis. *Sci. Rep.* 3:2606. <https://doi.org/10.1038/srep02606>.
23. Bretscher, M. S. 1984. Endocytosis: relation to capping and cell locomotion. *Science*. 224:681–686. <https://doi.org/10.1126/science.6719108>.
24. Kucik, D. F., S. C. Kuo, E. L. Elson, and M. P. Sheetz. 1991. Preferential attachment of membrane glycoproteins to the cytoskeleton at the leading edge of lamella. *J. Cell Biol.* 114:1029–1036. <https://doi.org/10.1083/jcb.114.5.1029>.
25. Schmidt, C. E., A. F. Horwitz, ..., M. P. Sheetz. 1993. Integrin-cytoskeletal interactions in migrating fibroblasts are dynamic, asymmetric, and regulated. *J. Cell Biol.* 123:977–991. <https://doi.org/10.1083/jcb.123.4.977>.
26. DiMilla, P. A., K. Barbee, and D. A. Lauffenburger. 1991. Mathematical model for the effects of adhesion and mechanics on cell migration speed. *Biophys. J.* 60:15–37. [https://doi.org/10.1016/S0006-3495\(91\)82027-6](https://doi.org/10.1016/S0006-3495(91)82027-6).
27. Kanchanawong, P., G. Shtengel, ..., C. M. Waterman. 2010. Nanoscale architecture of integrin-based cell adhesions. *Nature*. 468:580–584. <https://doi.org/10.1038/nature09621>.
28. Lee, J., and K. Jacobson. 1997. The composition and dynamics of cell-substratum adhesions in locomoting fish keratocytes. *J. Cell Sci.* 110:2833–2844. <https://doi.org/10.1242/jcs.110.22.2833>.
29. Choi, C. K., M. Vicente-Manzanares, ..., A. R. Horwitz. 2008. Actin and α -actinin orchestrate the assembly and maturation of nascent adhesions in a myosin II motor-independent manner. *Nat. Cell Biol.* 10:1039–1050. <https://doi.org/10.1038/ncb1763>.
30. Sarkar, A., D. N. LeVine, ..., X. Wang. 2020. Cell migration driven by self-generated integrin ligand gradient on ligand-labile surfaces. *Curr. Biol.* 30:4022–4032.e5. <https://doi.org/10.1016/j.cub.2020.08.020>.
31. Ezratty, E. J., C. Bertaux, ..., G. G. Gundersen. 2009. Clathrin mediates integrin endocytosis for focal adhesion disassembly in migrating cells. *J. Cell Biol.* 187:733–747. <https://doi.org/10.1083/jcb.200904054>.
32. Kaverina, I., O. Krylyshkina, and J. V. Small. 1999. Microtubule targeting of substrate contacts promotes their relaxation and dissociation. *J. Cell Biol.* 146:1033–1044. <https://doi.org/10.1083/jcb.146.5.1033>.
33. Balaban, N. Q., U. S. Schwarz, ..., B. Geiger. 2001. Force and focal adhesion assembly: a close relationship studied using elastic micropatterned substrates. *Nat. Cell Biol.* 3:466–472. <https://doi.org/10.1038/35074532>.
34. Broussard, J. A., D. J. Webb, and I. Kaverina. 2008. Asymmetric focal adhesion disassembly in motile cells. *Curr. Opin. Cell Biol.* 20:85–90. <https://doi.org/10.1016/j.ceb.2007.10.009>.
35. Kuo, J.-C., X. Han, ..., C. M. Waterman. 2011. Analysis of the myosin-II-responsive focal adhesion proteome reveals a role for β -Pix in negative regulation of focal adhesion maturation. *Nat. Cell Biol.* 13:383–393. <https://doi.org/10.1038/ncb2216>.
36. Hu, K., L. Ji, K. T. Applegate, ..., C. M. Waterman-Storer. 2007. Differential transmission of actin motion within focal adhesions. *Science*. 315:111–115. <https://doi.org/10.1126/science.1135085>.
37. Bate, N., A. R. Gingras, ..., D. R. Critchley. 2012. Talin contains a C-terminal Calpain2 cleavage site important in focal adhesion dynamics. *PLoS One*. 7:e34461. <https://doi.org/10.1371/journal.pone.0034461>.
38. Barnhart, E., K.-C. Lee, ..., A. Mogilner. 2015. Balance between cell–substrate adhesion and myosin contraction determines the frequency of motility initiation in fish keratocytes. *Proc. Natl. Acad. Sci. USA*. 112:5045–5050. <https://doi.org/10.1073/pnas.1417257112>.
39. Lee, J., A. Ishihara, ..., K. Jacobson. 1999. Regulation of cell movement is mediated by stretch-activated calcium channels. *Nature*. 400:382–386. <https://doi.org/10.1038/22578>.
40. Giannone, G., P. Rondé, ..., K. Takeda. 2004. Calcium rises locally trigger focal adhesion disassembly and enhance residency of focal adhesion kinase at focal adhesions. *J. Biol. Chem.* 279:28715–28723. <https://doi.org/10.1074/jbc.M404054200>.
41. Ji, L., J. Lim, and G. Danuser. 2008. Fluctuations of intracellular forces during cell protrusion. *Nat. Cell Biol.* 10:1393–1400. <https://doi.org/10.1038/ncb1797>.
42. Oliver, T., M. Dembo, and K. Jacobson. 1999. Separation of propulsive and adhesive traction stresses in locomoting keratocytes. *J. Cell Biol.* 145:589–604. <https://doi.org/10.1083/jcb.145.3.589>.
43. Rape, A. D., W. H. Guo, and Y. L. Wang. 2011. The regulation of traction force in relation to cell shape and focal adhesions. *Biomaterials*. 32:2043–2051. <https://doi.org/10.1016/j.biomaterials.2010.11.044>.
44. Oakes, P. W., S. Banerjee, ..., M. L. Gardel. 2014. Geometry regulates traction stresses in adherent cells. *Biophys. J.* 107:825–833. <https://doi.org/10.1016/j.bpj.2014.06.045>.
45. Bergert, M., A. Erzberger, ..., E. K. Paluch. 2015. Force transmission during adhesion-independent migration. *Nat. Cell Biol.* 17:524–529. <https://doi.org/10.1038/ncb3134>.
46. Beningo, K. A., M. Dembo, ..., Y. L. Wang. 2001. Nascent focal adhesions are responsible for the generation of strong propulsive forces in migrating fibroblasts. *J. Cell Biol.* 153:881–888. <https://doi.org/10.1083/jcb.153.4.881>.
47. Munevar, S., Y. Wang, and M. Dembo. 2001. Traction force microscopy of migrating normal and H-ras transformed 3T3 fibroblasts. *Biophys. J.* 80:1744–1757. [https://doi.org/10.1016/S0006-3495\(01\)76145-0](https://doi.org/10.1016/S0006-3495(01)76145-0).

48. Jurado, C., J. R. Haserick, and J. Lee. 2005. Slipping or gripping? Fluorescent speckle microscopy in fish keratocytes reveals two different mechanisms for generating a retrograde flow of actin. *Mol. Biol. Cell.* 16:507–518. <https://doi.org/10.1091/mbc.e04-10-0860>.
49. Gardel, M. L., B. Sabass, ..., C. M. Waterman. 2008. Traction stress in focal adhesions correlates biphasically with actin retrograde flow speed. *J. Cell Biol.* 183:999–1005. <https://doi.org/10.1083/jcb.200810060>.
50. Fournier, M. F., R. Sauser, ..., A. B. Verkhovskiy. 2010. Force transmission in migrating cells. *J. Cell Biol.* 188:287–297. <https://doi.org/10.1083/jcb.200906139>.
51. Guo, M., A. J. Ehrlicher, ..., D. A. Weitz. 2014. Probing the stochastic, motor-driven properties of the cytoplasm using force spectrum microscopy. *Cell.* 158:822–832. <https://doi.org/10.1016/j.cell.2014.06.051>.
52. Grashoff, C., B. D. Hoffman, ..., M. A. Schwartz. 2010. Measuring mechanical tension across vinculin reveals regulation of focal adhesion dynamics. *Nature.* 466:263–266. <https://doi.org/10.1038/nature09198>.
53. Meng, F., and F. Sachs. 2011. Visualizing dynamic cytoplasmic forces with a compliance-matched FRET sensor. *J. Cell Sci.* 124:261–269. <https://doi.org/10.1242/jcs.071928>.
54. Allen, G. M., K. C. Lee, ..., A. Mogilner. 2020. Cell mechanics at the rear act to steer the direction of cell migration. *Cell Syst.* 11:286–299.e4. <https://doi.org/10.1016/j.cels.2020.08.008>.
55. Roy, P., Z. Rajfur, ..., K. Jacobson. 2001. Local photorelease of caged Thymosin β 4 in locomoting keratocytes causes cell turning. *J. Cell Biol.* 153:1035–1048. <https://doi.org/10.1083/jcb.153.5.1035>.
56. Graziano, B. R., D. Gong, ..., O. D. Weiner. 2017. A module for Rac temporal signal integration revealed with optogenetics. *J. Cell Biol.* 216:2515–2531. <https://doi.org/10.1083/jcb.201604113>.
57. Graham, D. M., L. Huang, ..., M. A. Messerli. 2013. Epidermal keratinocyte polarity and motility require Ca^{2+} influx through TRPV1. *J. Cell Sci.* 126:4602–4613. <https://doi.org/10.1242/jcs.122192>.
58. Xia, N., C. K. Thodeti, ..., D. E. Ingber. 2008. Directional control of cell motility through focal adhesion positioning and spatial control of Rac activation. *FASEB J.* 22:1649–1659. <https://doi.org/10.1096/fj.07-090571>.
59. Johnson, H. E., S. J. King, ..., J. M. Haugh. 2015. F-actin bundles direct the initiation and orientation of lamellipodia through adhesion-based signaling. *J. Cell Biol.* 208:443–455. <https://doi.org/10.1083/jcb.201406102>.
60. Welf, E. S., S. Ahmed, ..., J. M. Haugh. 2012. Migrating fibroblasts reorient directionality by a metastable, PI3K-dependent mechanism. *J. Cell Biol.* 197:105–114. <https://doi.org/10.1083/jcb.201108152>.
61. Andrew, N., and R. H. Insall. 2007. Chemotaxis in shallow gradients is mediated independently of PtdIns 3-kinase by biased choices between random protrusions. *Nat. Cell Biol.* 9:193–200. <https://doi.org/10.1038/ncb1536>.
62. Van Haastert, P. J. M. 2010. Chemotaxis: insights from the extending pseudopod. *J. Cell Sci.* 123:3031–3037. <https://doi.org/10.1242/jcs.071118>.
63. Petrie, R. J., and K. M. Yamada. 2012. At the leading edge of three-dimensional cell migration. *J. Cell Sci.* 125:5917–5926. <https://doi.org/10.1242/jcs.093732>.
64. Diz-Muñoz, A., P. Romanczuk, ..., E. K. Paluch. 2016. Steering cell migration by alternating blebs and actin-rich protrusions. *BMC Biol.* 14:74. <https://doi.org/10.1186/s12915-016-0294-x>.
65. Fritz-Laylin, L. K., M. Riel-Mehan, ..., R. D. Mullins. 2017. Actin-based protrusions of migrating neutrophils are intrinsically lamellar and facilitate direction changes. *Elife.* 6:e26990. <https://doi.org/10.7554/eLife.26990>.
66. Labuz, E. C., M. J. Footer, and J. A. Theriot. 2023. Confined keratocytes mimic in vivo migration and reveal volume-speed relationship. *Cytoskeleton.* 80:34–51. <https://doi.org/10.1002/cm.21741>.
67. Callan-Jones, A. 2022. Self-organization in amoeboid motility. *Front. Cell Dev. Biol.* 10:1000071. <https://doi.org/10.3389/fcell.2022.1000071>.
68. Liu, Y.-J., M. Le Berre, ..., M. Piel. 2015. Confinement and low adhesion induce fast amoeboid migration of slow mesenchymal cells. *Cell.* 160:659–672. <https://doi.org/10.1016/j.cell.2015.01.007>.
69. Kapustina, M., T. C. Elston, and K. Jacobson. 2013. Compression and dilation of the membrane-cortex layer generates rapid changes in cell shape. *J. Cell Biol.* 200:95–108. <https://doi.org/10.1083/jcb.201204157>.
70. Sugimura, K., and S. Ishihara. 2013. The mechanical anisotropy in a tissue promotes ordering in hexagonal cell packing. *Development.* 140:4091–4101. <https://doi.org/10.1242/dev.094060>.
71. Treppe, X., M. R. Wasserman, ..., J. J. Fredberg. 2009. Physical forces during collective cell migration. *Nat. Phys.* 5:426–430. <https://doi.org/10.1038/nphys1269>.
72. Yamaguchi, N., Z. Zhang, ..., H. Knaut. 2022. Rear traction forces drive adherent tissue migration in vivo. *Nat. Cell Biol.* 24:194–204. <https://doi.org/10.1038/s41556-022-00844-9>.
73. Mierke, C. T., D. Rösel, ..., J. Brábek. 2008. Contractile forces in tumor cell migration. *Eur. J. Cell Biol.* 87:669–676. <https://doi.org/10.1016/j.ejcb.2008.01.002>.
74. Fraley, S. I., Y. Feng, ..., D. Wirtz. 2010. A distinctive role for focal adhesion proteins in three-dimensional cell motility. *Nat. Cell Biol.* 12:598–604. <https://doi.org/10.1038/ncb2062>.
75. O'Neill, P. R., J. A. Castillo-Badillo, ..., N. Gautam. 2018. Membrane flow drives an adhesion-independent amoeboid cell migration mode. *Dev. Cell.* 46:9–22.e4. <https://doi.org/10.1016/j.devcel.2018.05.029>.